Jurnal
Teknologi

Full Paper

STUDY OF CO_2 ADSORPTION AND DESORPTION ON ACTIVATED CARBON SUPPORTED IRON OXIDE BY TEMPERATURE PROGRAMMED DESORPTION

Azizul Hakim[a]*, Maratun Najiha Abu Tahari[a], Tengku Sharifah Marliza[a], Wan Nor Roslam Wan Isahak[b], Muhammad Rahimi Yusop[b], Mohamed Wahab Mohamed Hisham[b], Mohd. Ambar Yarmo[a]

[a]UKM Catalysis Research Group, School of Chemical Sciences and Food Technology, Faculty of Science and Technology, Universiti Kebangsaan Malaysia, 43600 UKM, Bangi, Malaysia
[b]Department of Chemical and Process Engineering, Faculty of Engineering and Built Environment, Universiti Kebangsaan Malaysia, 43600 UKM, Bangi, Malaysia

Article history
Received
15 July 2015
Received in revised form
1 October 2015
Accepted
25 October 2015

*Corresponding author
azizulhakim2442@gmail.com

Graphical abstract

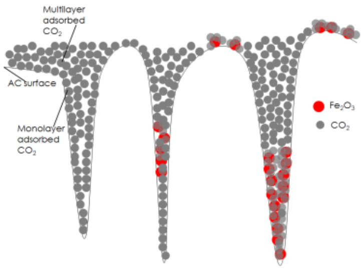

CO_2 adsorption on xFe_2O_3/AC diagram

Abstract

Anthropogenic gas of CO_2 level was higher than CO_2 atmospheric safety limit of 350 ppm since 80's. It can be assumed that CO_2 level growth directly proportional to the population and development. Hence, studies on CO_2 capture have been extensively established in between year of 2000-2010. Metal oxide can be a good adsorbent but it has the weakness in surface area and sintered after regeneration process. Thus, activated carbon was used to enhance the surface area which mainly responsible for physical adsorption. Fe_2O_3 supported on activated carbon (Fe_2O_3/AC) were prepared by impregnation method and used for CO_2 adsorption-desorption studies. The XRD result shows that precursor of ferric nitrate used to impregnated on AC (activated carbon) support was directly dissociated to Fe_2O_3 metal oxide by thermal treatment under N_2 atmosphere temperature at 450 °C. The loading amount of Fe_2O_3 by weight ratio affect the textural properties and CO_2 capturing capacity. The surface area and pore volume of the catalyst decrease with the loading of Fe_2O_3. Highest Fe_2O_3 loading shows greater amount chemically adsorbed of CO_2. Nevertheless, it drastically reduced the surface area of the AC, which is chiefly responsible for CO_2 physisorption, thus decreasing the carrying capacity of ACs at 25 °C. The $20Fe_2O_3$/AC was found to be optimum loading for better physi and chemisorptions of CO_2.

Keywords: Adsorption; iron oxide; activated carbon; carbon dioxide

Abstrak

Peningkatan gas antropogen seperti CO_2 telah pun melebihi tahap keselamatan atmosfera iaitu 350 ppm semenjak tahun 80-an. Peningkatan CO_2 boleh dianggap berkadar langsung dengan populasi dan pembangunan. Oleh sedemikian, kajian dalam bidang ini telah meningkat di antara tahun 2000-2010. Logam oksida merupakan penjerap yang baik, namun ia mempunyai kelemahan dari segi ciri luas permukaan dan menjadi sinter selepas proses penghasilan semula. Dengan menggunakan karbon aktif (AC) sebagai penyokong, boleh mempertingkatkan luas permukaan penjerap yang memainkan peranan penting dalam penjerapan sacara fizikal. Fe_2O_3 yang disokong pada karbon aktif (Fe_2O_3/AC) disediakan dengan kaedah impregnasi atau pengisitepuan, seterusnya digunakan dalam kajian penjerapan-penyahjerapan CO_2. Keputusan XRD menunjukkan ferum nitrat yang disokong pada AC telah dileraikan kepada logam oksida, Fe_2O_3, dengan pemanasan yang dialirkan N_2 pada suhu 450 °C. Jumlah muatan Fe_2O_3 yang berdasarkan nisbah jisim memberi kesan pada ciri teksturnya dan keupayaan penjerapan CO_2. Luas permukaan dan isi padu liang pemangkin berkurangan dengan penambahan muatan Fe_2O_3 pada penyokong. Muatan Fe_2O_3 yang tinggi menunjukkan peningkatan jumlah CO_2 yang dijerap secara kimia. Walaubagaimanapun, ia memberi kesan penurunan luas permukaan karbon aktif secara mendadak, dimana ia memainkan peranan utama dalam pejerapan secara fizikal. Oleh sedemikian, ia merendahkan keupayaan penjerapan yang rendah karbon aktif tersebut pada suhu 25 °C. Kajian ini mendapati sampel $20Fe_2O_3$/AC merupakan muatan optimum untuk penjerapan CO_2 yang lebih berkesan dari segi fizikal dan kimia.

Kata kunci: Penjerapan; ferum oksida; karbon aktif; karbon dioksida

1.0 INTRODUCTION

Green house gas of CO_2 level increase with average growth rate of 2.0 ppm/year and has been away further from CO_2 atmospheric safety limit of 350 ppm since 80's [1]. Considerable attentions were paid to CO_2 capturing by adsorption and desorption CO_2 as regeneration to fully utilize the abundance of anthropogenic gas. A numbers of research were done with varies carbon capture technologies, for instance sorbents, solvent and membrane [2].

Adsorbents properties mainly related to the adsorbed particles (molecular size, molecular weight and polarity) and its surface (polarity, pore size and spacing) determine the adsorption quality. The exothermic process for adsorption requiring temperature, in order to regenerate the adsorbents through desorption. Solid sorbents have the potential for significant energy savings over liquid solvents, in part because they avoid the need for the large quantities of water that must be repeatedly heated and cooled to regenerate the solvent solution [3].

Adsorption CO_2 by solid sorbent of metal oxides, calcium oxide (CaO) was among earliest material used as adsorbent. Its capability in high CO_2 adsorption and high raw material availability (e.g. limestone) at a low cost but the CO_2 desorption required high energy (800 °C) [4]. Sintering through the carbonation/calcination cycle which reduces the adsorbent's pore volume and surface area [5] give rises to discovering materials that could overcome these problems.

Early studies formation of carbonate species on hematite, (Fe_2O_3) has been carried out using vibrational spectroscopy which only symmetrical carbonate stretch was detected [6]. Progressively, it was interesting to noted that several carbonate species of monodentate, bidentate, bicarbonate and carboxylate interacted on Fe_2O_3 surface as complexes [7, 8].

CO_2 interaction mechanism on iron oxide has been proposed by bargar as shown in Fig. 1, with comparison experimental and calculated frequencies of different carbonate species [8]. Highly sensitive of vibration frequencies to the structures, protonation states, and coordination environments of carbonate, and thus provide an excellent probe to determine the compositions and structures of carbonate adsorbed at water-hematite interfaces. However, practically was difficult to assigning the molecular structure. In solid form, carbonate coordination including mono-, bi-, tri-, and tetranuclear monodentate complexes, mono- and binuclear bidentate complexes, and combinations thereof [8]. In addition, carbonate can exhibit extensive hydrogen bonding to neighboring interference of water molecules and OH groups. Ramis et. al reported that CO_2 adsorption at low temperature of 173 and 273 K resulted linearly coordinated CO_2 and bent adsorbed CO_2 is likely intermediate of bicarbonate species [9].

The CO_2 adsorbed chemically and physically on metal oxides are based on acid base and its surface properties respectively. The CO_2 chemisorption involves basic sites that act as electron donors are associated with O^{2-} ions localized on surface defects [10]. Ferretto et. al works focus on CO_2 exposure on hematite at atmospheric pressure as well as under high vacuum condition and may interact with the powder sample either reacting with surface OH groups giving rise to bicarbonate species, or with surface cations and neighbouring oxide ions to originate bidentate carbonate species [11].

Carbonaceous type adsorbents such as activated carbon (AC) [12] have been widely used for CO_2 capture. It has favourable properties for gas sorption because of wide availability, low cost, high thermal stability and low sensitivity to moisture, their application is limited to treat high pressure gases. The weak CO_2 desorption of carbonaceous materials in a range of 100 °C leads to favourable in low energy consumption in operation. However, CO_2 adsorption on AC only involved weak interaction by physisorption. Modification of the AC surface by loaded with iron oxide, Fe_2O_3 expecting certain iron oxide loading percentage provide improvement especially in chemisorption.

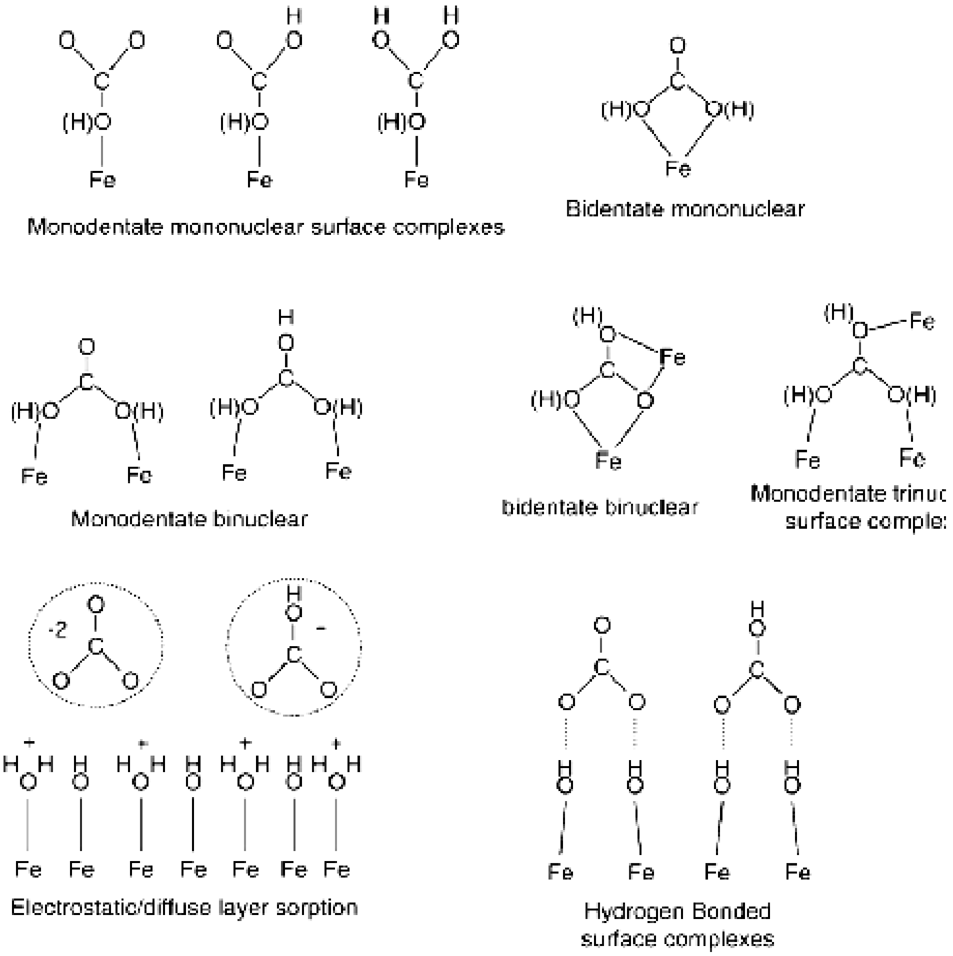

Figure 1 Interactions of carbonate species formed on Fe_2O_3 surfaces. Dashed lines represents hydorgen bonding where it could be from bicarbonate or hydrogen bonded carbonate complex closely associated with Fe_2O_3 surface. The electrostatic/diffuse layer sorption was also determined as minor complex that dependant on pH.

As a consequence, current research focus on how to improve the CO_2 adsorption capacity by physically and chemically adsorbed via two ways, to improve surface area and pore structure of the carbonaceous adsorbents either using different precursors and to increase basicity by chemical modification on surface. This study will emphasize CO_2 adsorption-desorption of Fe_2O_3 on AC to enhance the surface area feature by temperature programmed desorption (TPD).

2.0 EXPERIMENTAL

2.1 Samples Preparation

Charcoal AC and iron (III) nitrate nonahydrate ($Fe(NO_3)_2.9H_2O$) were purchased from QreC, Malaysia and Sigma Aldrich, USA respectively. Bulk Fe_2O_3 obtained from BDH was used treatment as a reference. Supported Fe_2O_3 catalysts were prepared by a conventional impregnation method. The desired amount of $Fe(NO_3)_2.9H_2O$ firstly dissolved in a mixed solution of 30 g distilled water and 10 g ethanol at room temperature. The AC obtained without further treatment was added to the solution and stirred for 24 hours at room temperature. The mixture was directly evaporated at 85 °C and further dried at 110 °C for 10 hours in the oven. The dried samples were heated under thermal treatment with N_2 atmosphere to 450 °C and held for 1 hour under N_2 atmosphere. The resultant samples were denoted as xFe_2O_3/AC (x is the percentage by mass).

2.2 Characterization

The X-ray Diffraction (XRD, Bruker AXS D8 Advance) patterns obtained were matched with standard diffraction data (JCPDS) file for identification of crystalline phase composition. N_2 adsorption-desorption was conducted in a Micromeritics ASAP 2020 instrument to determine the textural surface properties. The sample was outgassed at 200 °C for 6 hours prior to adsorption. The surface area calculated by Brunauer–Emmett–Teller (BET) method, while t-plot method was used to calculate the micropore volume (V_{mic}) and micropore surface area (S_{mic}).

2.3 CO_2 Adsorption And Desorption

The CO_2 adsorption behaviors was identified using purified CO_2 (99.9%) at 25 °C was applied using same instrument and degassed method mentioned previously in 2.1. CO_2–TPD was performed using Chemisorption Analyzer type Micrometics 2920 Chemisorb. 50 mg samples were preheated to 150 °C to remove the moisture content before the mixture gas of 5 % CO_2 in He was introduced in a constant temperature of 40 °C for 60 minutes. The excess weak physically adsorbed CO_2 was removed by exposed with pure He at 50 °C and TPD begin heated to 900 °C under pure He.

3.0 RESULTS AND DISCUSSION

3.1 Characterization

The AC exhibited common characteristic broad peaks of the graphitic structure with 2θ being 26° and 43°, and these diffraction peaks become weaker with the increased of the metal loadings as shown in Fig. 2. The typical peaks for Fe_2O_3 gradually increase on the amorphous peak with the Fe_2O_3 content in the AC support. The XRD pattern of Fe_2O_3 have all the diffraction peaks can be indexed to a rhombohedral phase a-Fe_2O_3 with lattice parameters a = 5.03 and c = 13.76 (JCPDS, 01-077-9927). Additionally, some peaks ascribed to carbolite structure with high intensity at 60Fe_2O_3/AC with 2θ being 26.6° was detected. This peak ascribed from quenching high temperature carbon onto metal substrate [13]. The diffraction peaks of 60Fe_2O_3/AC were detected mainly attributed to Fe_2O_3 in the XRD patterns with several peaks shifted ascribed to the Fe_2O_3 well dispersed in the AC's pore. Thermal treatment at 450 °C under N_2 atmosphere were found that nitrate compounds were dissociated completely since $Fe(NO_3)_2.9H_2O$ decomposed at 250 °C formed Fe_2O_3 [14]. During thermal treatment under N_2 atmosphere, it was observed that toxic brown gas of nitrogen dioxide (NO_2) evolved in the sample tube. It is interesting to observed that higher intensity of brown gas evolved with high metal loading due to $Fe(NO_3)_2.9H_2O$ contained.

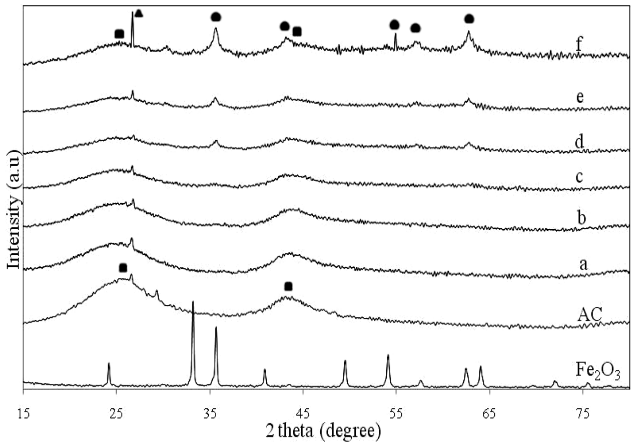

Figure 2 XRD patterns of the a) 5Fe_2O_3/AC, b) 10Fe_2O_3/AC, c) 20Fe_2O_3/AC, d) 30Fe_2O_3/AC, e) 40Fe_2O_3/AC and f) 60Fe_2O_3/AC, where (●) is Fe_2O_3, (▲) is carbolite and (■) is AC.

The N_2 adsorption-desorption isotherms of xFe_2O_3/AC exhibits Type I isotherm (Fig. 3) in the IUPAC classification, with steep initial region due to strong adsorption shows a typical microporous materials. These isotherms with type H4 hysteresis underlying Type I isotherm and had been associated with porous materials that parallel over a wide range of relative pressure which exhibiting a narrow slit-shaped pores of mesopores [15]. The mesopores formation is thought that Fe_2O_3 accelerates burning off of carbon wall and enlarging pore sizes during the thermal treatment. The adsorption amount of xFe_2O_3/AC generally decreases with increasing metal loadings except for 20Fe_2O_3/AC appear highest (880.2 m^2/g) among all adsorbents (Table 1). This profile is indicate that macropores of the support are blocked or covered at higher metal loading, which led to decrease of surface area. The change in the metal loading may result in a formation of maximum in the surface area of the catalyst. The 20Fe_2O_3/AC sample with higher surface area has in the agreement that reported by Aksoylu et. al, where the maximum loading for above 15 wt % formed its own porous structure on the catalyst surface [16]. The Fe_2O_3 prepared as shown in the inset of Fig. 3 shows Type III isotherm ascribed from the weak adsorbate-adsorbent interaction with H3 hysterisis that indicative the presence of mesoporous and macroporous on its surface. Hence, it determined the plate-like particles which give rise to slit-shaped pores.

The pore size distribution for AC microporous samples were computed using density functional theory (DFT) method for accurate micropore filling mechanism as shown in Fig. 4 [17]. Meanwhile, pore size distribution for Fe_2O_3 sample was computed by Berret, Joyner, Halenda (BJH) method for mesoporous and macroporous materials. None of the ACs were containing larger pore was produced. The AC sample shows narrow and deep pore volume and its deepness reduction was mainly attributed by additive of Fe_2O_3 that modified AC's surface to increase its basicity. The Fe_2O_3 tends to filled the deepest part of the pores that significantly in shorten pores depth and remains the pore diameter as shown in Fig. 4. Increament percentage by weight of Fe_2O_3 loading does not affect pore diameter. As for Fe_2O_3 sample, larger pore size distribution range that covered mesoporous (20-500Å) and mostly macroporous (>500 Å) indicate poor adsorption properties.

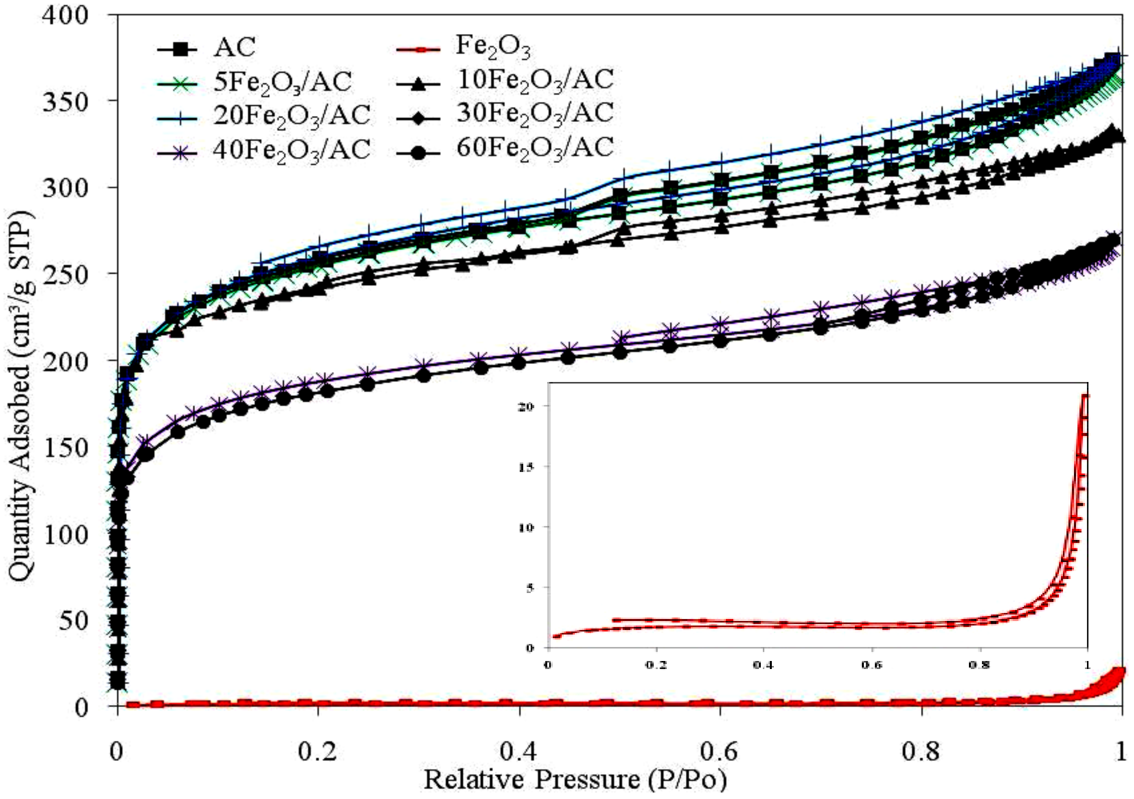

Figure 3 The nitrogen adsorption/desorption isotherms of the catalysts.

Table 1 The textural characteristics and adsorption properties of xFe_2O_3/AC

Samples	**Surface area**		**Pore volume**		**Pore diameter (nm)**	**99.9% CO_2 adsorption at 25 °C**	
	S_{BET} [a] (m^2/g)	**S_{mic} [b] (m^2/g)**	**V_{tot} [c] (cm^3/g)**	**V_{mic} [d] (cm^3/g)**		**(cm^3/g)**	**$(mg_{CO_2}/g_{adsorbent})$**
AC	862.7	483.3	0.57	0.23	2.6	58.67	115.2
Fe_2O_3	5.7	1.77	0.02	9×10^{-4}	15.4	1.53	3.0
$5Fe_2O_3/AC$	858.4	478.4	0.56	0.23	2.6	50.68	99.6
$10Fe_2O_3/AC$	807.3	463.4	0.51	0.22	2.5	48.16	94.6
$20Fe_2O_3/AC$	880.2	486.8	0.57	0.23	2.6	52.77	103.7
$30Fe_2O_3/AC$	800.1	460.7	0.49	0.22	2.4	47.18	92.7
$40Fe_2O_3/AC$	630.9	360.0	0.41	0.17	2.6	42.88	84.2
$60Fe_2O_3/AC$	611.9	318.3	0.42	0.15	2.7	42.25	83.0

[a] Surface area by BET method.
[b] Micropore surface area by T-plot method.
[c] Single point total pore volume.
[d] Micropore volume by T-plot method.

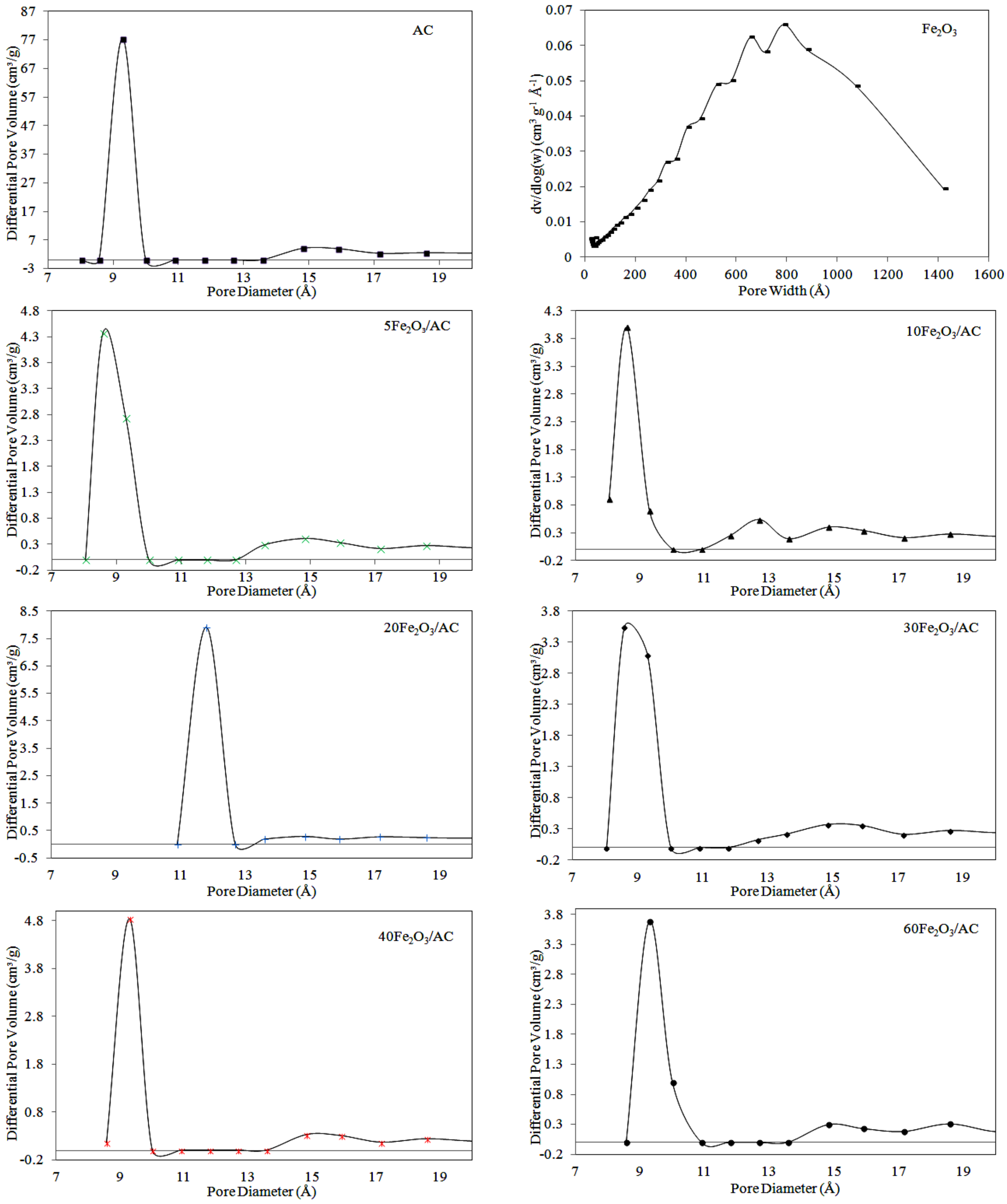

Figure 4 The pore size distribution of adsorbents.

3.2 Physical Phenomenon of CO_2 Adsorption

The CO_2 adsorption isotherms at 25 °C were varies for xFe_2O_3/AC with different metal loadings (Fig. 5). The CO_2 adsorption isotherm at 25 °C for AC shows the highest CO_2 adsorption capacity of 115.2 $mg_{CO_2}/g_{adsorbent}$ (58.67 cm^3) while $20Fe_2O_3$/AC exhibited slightly lower than AC at 50.68 cm^3/g (99.6 $mg_{CO_2}/g_{adsorbent}$). The $60Fe_2O_3$/AC has lowest CO_2 adsorption because of low surface area, as a consequence of high metal loading. The empty pores of AC have the space for capturing adsorbate of CO_2. However, the metal loading cause pores become shallow, hence less space for CO_2 to be trapped. In order to enhance the physical adsorption capacity, modification by increase adsorbent's basicity with metal loading. Fe_2O_3 has the ability as metal oxide

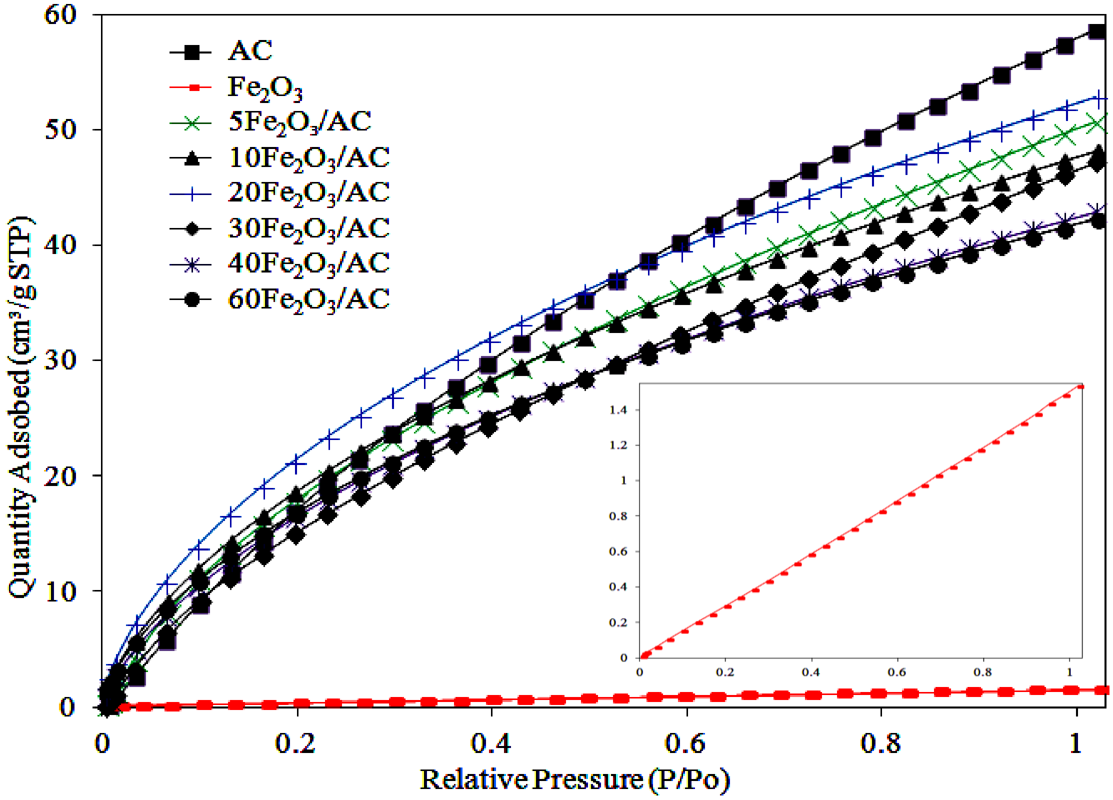

Figure 5 CO_2 adsorption isotherms at 25 °C.

that attracts CO_2 formed metal carbonate. The CO_2 adsorption for Fe_2O_3 was 1.53 cm³/g (3.0 $mg_{CO_2}/g_{adsorbent}$), with poor surface area that existence of mesopores and macropores on its surface.

The major contributing factor of physisorption mechanism is chiefly on the morphology of the adsorbent.The empty pores of AC easily filled with CO_2 which begin with monolayer of CO_2 adsorbed and followed by multilayer adsorption of CO_2 (Fig. 6). After impregnation, the AC pores filled with Fe_2O_3 and same mechanism of physisorption occurred with addition of chemical interaction formed on the Fe_2O_3 surface as carbonate complexes.

Fe_2O_3 that filled in the AC's pores reduces the space for CO_2 to be trapped but it created carbonate formation on Fe_2O_3 surfaces that could improve in chemisorption as well. As a result, this condition improved the CO_2 adsorption in both ways of physi and chemisorption. For higher Fe_2O_3 loading on AC, more Fe_2O_3 particles filled the pores and CO_2 attracted by acid base properties. Thus, CO_2 adsorption was considerable possessed by chemisorptions instead of physisorption. Chemically adsorbed CO_2 require higher energy to dissociate carbonate complexes formed. The CO_2-TPD analysis was carried out in order to correlate the metal loading with chemically adsorbed CO_2.

3.3 Regeneration Process of CO_2 Study

TPD analysis was carried out by measuring the amount of CO_2 desorbed results of the sorbent after CO_2 exposure. Besides adsorption capacity, the regeneration property where chemically bonded as CO_3^{2-} and releases as CO_2 by thermally decomposition is one of the most important factors to be considered. This chemical phenomenon was investigated in order to study the maximum desorption temperature. According to thermal desorption theory, pre-treated sample heated at an increasing temperature with constant rate with inert gas flow such as helium, argon or nitrogen [18]. Stronger chemisorption correlated with the strong is the bond which require higher temperature desorption.

In the case of xFe_2O_3/AC, most of chemically bonded CO_3^{2-} releases as CO_2 at maximum temperature of 656.0 °C except $5Fe_2O_3/AC$ has another major peak at 721.6 °C indicative of the Fe_2O_3 located deep in the pore led to harder CO_2 released as shown in Fig. 7. The chemically adsorbed CO_2 was increased gradually with increases of Fe_2O_3 loading (Table 2).

AC supported Fe_2O_3 provides an enhancement in surface area that desirable in CO_2 adsorption. Hence, this chemical phenomenon derives a direct proportional relationship between metal loading via

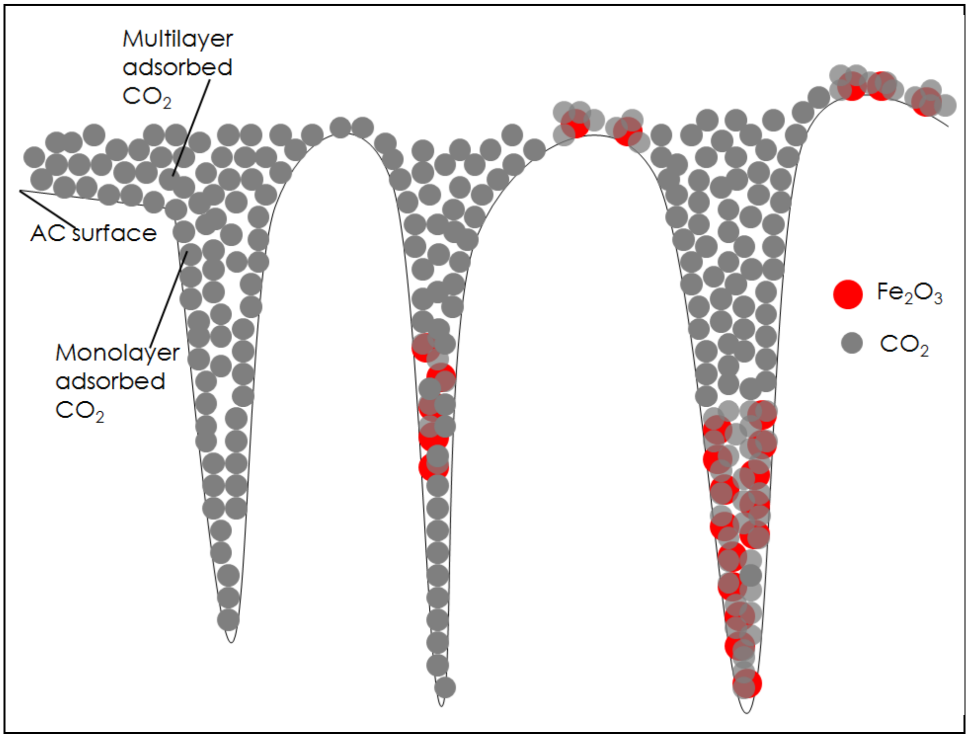

Figure 6 Physically adsorbed CO_2 at 25 °C mechanism. Transparent color represent CO_2 that chemically bonded with Fe_2O_3.

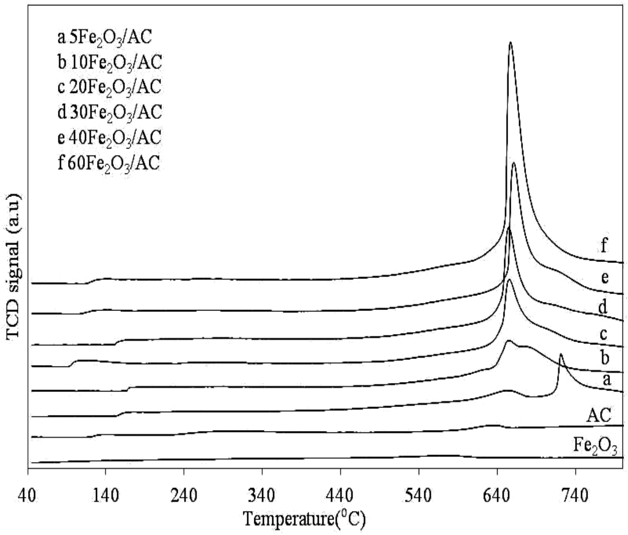

Figure 7 CO_2-TPD profiles for xFe_2O_3/AC catalysts.

Table 2 CO_2 adsorption capacity by CO_2–TPD analysis using mixture gas of 5% CO_2 in He.

Samples	**5% CO_2-TPD**	
	(cm^3/g)	**(mg_{CO_2} / $g_{adsorbent}$)**
AC	8.87	17.4
Fe_2O_3	1.94	3.8
$5Fe_2O_3/AC$	33.32	65.5
$10Fe_2O_3/AC$	48.51	95.3
$20Fe_2O_3/AC$	53.03	104.2
$30Fe_2O_3/AC$	67.00	131.6
$40Fe_2O_3/AC$	72.88	143.2
$60Fe_2O_3/AC$	90.58	177.9

chemical adsorptive capacity. The bulk Fe_2O_3 with low surface area led to low adsorption capacity of 3.8 mg_{CO_2}/ $g_{adsorbent}$. The active site of bulk Fe_2O_3 was significantly less compared to supported with AC. It is due to agglomeration of the bulk Fe_2O_3 particles substantially reduced its surface area as well as its active site that responsible to attract CO_2.

The catalysts exhibit strong interaction between monolayer adsorbed of CO_2 and Fe_2O_3 surface that require temperature for desorption purpose. Even though the adsorption capacity was lower than common adsorbent CaO, however it has better features in physi and chemisorption behavior.

This work was higher in adsorption capacity compared to previous research of nickel oxide supported on AC with 20NiO/AC was only 37.0 mg_{CO_2}/ $g_{adsorbent}$ [19]. In comparison with chemically modified of monoethanolamine (MEA) on kenaf core fibre into AC, 10 % of loading was only adsorption capacity of 9.0 $mg_{CO_2}/g_{adsorbent}$ [20]. In fact, amine based adsorbent has the constraints in practical application because of its high vapor pressure which incurs high loss of ammonia in regeneration process and unlikely secondary reaction between CO_2 and amine groups formed a stable product, most likely urea, resulting reduced adsorption sites[21].

4.0 CONCLUSION

The CO_2 adsorption-desorption on developed adsorbents by conventional impregnation method and thermal treatment at 450 °C under N_2 atmosphere found that Fe_2O_3 particles well distributed with increased the intensities of crystallinity from XRD result. From the N_2 adsorption-desorption isotherms, the xFe_2O_3/AC indicated Type I isotherm and H3 hysterisis according to IUPAC classification. Type I isotherm was mainly contributed from the AC material which is highly microporous material, while H4 hysterisis ascribed from the Fe_2O_3 loading which exhibited mesoporous and macroporous on its surfaces. Pore size distribution by using DFT method was confirmed that increment of metal loading does not affecting the pore diameter since Fe_2O_3 particles were filled deep in the AC's pores. It can be proposed that higher metal loading easily formed with high tendency of agglomerated Fe_2O_3 In the AC's pores. Meanwhile, pore size distribution for bulk Fe_2O_3 by using BJH method proved that composed of mesoporous and macroporous structure. From the CO_2 adsorption isotherm at 25 °C, $20Fe_2O_3$/AC recorded highest efficiency with CO_2 adsorption capacity of 103.7 $mg_{CO_2}/g_{adsorbent}$. The physisorption mainly contributed by adsorbent surface. At higher Fe_2O_3 loading on AC, CO_2 adsorbed attracted by the Fe_2O_3 due to acid base properties which is now chemisorption plays an important role instead of physisorption. Thus, CO_2–TPD analysis was performed to prove this theory. These samples showed strong interactions with low CO_2 concentration as low as 5% in He. The CO_2-TPD provides the temperature profiles of the CO_3^{2-} ions that strongly chemical bonded dissociates at 656 °C as CO_2. The Fe_2O_3 loading increased the basicity of the adsorbent significantly enhance the CO_2 chemisorption. Furthermore, it was proven that higher Fe_2O_3 loading on AC increased its basicity and attracted more CO_2 to be chemically bonded as carbonate complexes. Nevertheless, higher metal loading exhibited lower surface area that chiefly responsible for the CO_2 physisorption. It is important to consider both physi and chemisorption that could enhance the adsorption capacity. Finally, $20Fe_2O_3$/AC was found to be optimum loading for better physi and chemisorption of CO_2.

Acknowledgement

The authors wish to thanks Universiti Kebangsaan Malaysia (UKM) for funding this project under research grants LRGS/BU/2011/USM-UKM/PG/02, BKBP-FST-K003323, ETP-2013-066 and TD-2014-024 from Ministry of Higher Education (MOHE) Malaysia. Appreciations to Centre of Research and Innovation Management (CRIM) and School of Chemical Science and Food Technology in UKM for the instruments facilities.

References

[1] Global Monitoring Division, National Oceanic and Atmospheric Administration, U.S. Department of Commerce. Acessed on 30 October 2014. ftp://aftp.cmdl.noaa.gov/products/trends/co2/co2_annmean_gl.txt.
[2] B. Y. Li, Y. H. Duan, D. Luebke, B. Morreale. 2013. Advances in CO_2 Capture Technology: A patent review. *Applied Energy*. 102: 1439-1447.
[3] J. D. Figueroa, T. Fout, S. Plasynki, H. McIlvried, R. D. Srivastaa. 2008. Advances in CO_2 Capture Technology—The U.S. Department of Energy's Carbon Sequestration Program. *International Journal of Greenhouse Gas Control*. 2: 9-20.
[4] S. Y. Lin, K. Takashi, Y. Wang and N. Katsuhiro. 2011. Energy Analysis of $CaCO_3$ Calcination with CO2 Capture. *Energy Procedia*. 4: 356-361.
[5] J. C. Abanades. 2002. The Maximum Capture Efficiency Of CO_2 Using A Carbonation/ Calcination Cycle Of $CaO/CaCO_3$. *Chemical Engineering Journal*. 90: 303-306.
[6] R.M. Taylor. 1980. Formation And Properties Of Fe (II) Fe (III) Hydroxyl-Carbonate And Its Possible Significance In Soil Formation. *Clay Minerals*. 15: 369-382.
[7] J. Baltrusaitis, J. Schuttlefield, E. Zeitler, V.H. Grassian. 2011. Carbon Dioxide Adsorption On Oxide Nanoparticle Surfaces. *Chemical Engineering Journal*. 170: 471-481.
[8] J. R. Bargar, J. D. Kubicki, R. Reitmeyer, J. A. Davis. 2005. ATR-FTIR Spectroscopic Characterization Of Coexisting Carbonate Surface Complexes On Hematite. *Geochimica et Cosmochimica Acta*. 69: 1527-1542.
[9] G. Ramis, G. Busca, V. Lorenzelli. 1991. Low-Temperature CO_2 Adsorption On Metal Oxides: Spectroscopic Characterization Of Some Weakly Adsorbed Species. *Materials Chemistry and Physics*. 29: 425-435.
[10] R. R. Kondakindi, G. McCumber, S. Aleksic, W. Whittenberger, M. A. Abraham. 2013. Na_2CO_3-Based Sorbents Coated On Metal Foil: CO_2 Capture Performance. *International Journal of Greenhouse Gas Control*. 15: 65-69.
[11] L. Ferretto, A. Glisenti. 2002. Study Of The Surface Acidity Of An Hematite Powder. *Journal of Molecular Catalysis A: Chemical*. 187: 119-128.
[12] M. G. Plaza, C. Pevida, J. J. Pis, F. Rubiera. 2011. Evaluation Of The Cyclic Capacity Of Low-Cost Carbon Adsorbents For Post-Combustion CO_2 Capture. *Energy Procedia*. 4: 1228-1234.
[13] S. Tanuma, V. Palnichenko', N. Satoh. 1995. Synthesis Of Low Density Carbon Crystals By Quenching Gaseous Carbon And Intercalation Of Alkali Metal Atoms Into These Crystals. *Synthetic Metals*. 71: 1841-1844.
[14] M. A. A. Elmasry, A. Gaber, E.M.H. Khater. 1998. Thermal Decomposition Of Ni (II) and Fe (III) Nitrates And Their Mixture. *Journal of Thermal Analysis and Calorimetry*. 52(2): 489-495.
[15] K. S. W. Sing, D. H. Everett, R.A.W. Haul, L. Moscou, R.A. Pierotti, J. Rouquerol, T. Siemieniewska. 1985. Reporting Physisorption Data For Gas/Solid Systems With Special

References To The Determination Of Surface Area And Porosity. Pure & Applied Chemistry. 57: 603-619.

[16] A. E. Aksoylu, A. N. Akin, Z.I. Onsan and D. L. Trimm. 1996. Structure/Activity Relationship In Coprecipitated Nickel-Alumina Catalysts Using CO_2 Adsorption And Methanation. *Applied Catalysis A: General*. 145: 185-193.

[17] J.B. Condon. 2006. *Surface Area And Porosity Determinations By Physisorption Measurements And Theory. First Edition*. UK: Elsevier.

[18] M. Fadoni, L. Lucarelli. 1998. Temperature Programmed Desorption, Reduction, Oxidation And Flow Chemisorptions For The Characterization Of Heterogeneous Catalysts. Theoritical Aspects, Instrumentation And Applications. *Studies in Surface Science and Catalysis*. 120: 177-225.

[19] A. Hakim, W. N. R. Wan Isahak, M. N. Abu Tahari, M. R. Yusop, M. W. Mohamed Hisham, M. A. Yarmo. 2015. Temperature Programmed Desorption Of Carbon Dioxide For Activated Carbon Supported Nickel Oxide: The Adsorption And Desorption Studies. *Advanced Materials Research*. 1087: 45-49.

[20] N. Zaini, K. S. Nor Kamarudin. 2014. Adsorption Of Carbon Dioxide On Monoethanolamine (MEA)–Impregnated Kenaf Core Fiber By Pressure Swing Adsorption System (PSA). *Jurnal Teknologi*. 5: 11-16.

[21] A. Sayari, Y. Belmabkhout, R. Serna-Guerrero. 2011. Flue gas Treatment Via CO_2 Adsorption. *Chemical Engineering Journal*. 171: 760-774.